LETTER

doi:10.1038/nature10453

Molecular mechanism of anaerobic ammonium oxidation

Boran Kartal[1], Wouter J. Maalcke[1], Naomi M. de Almeida[1], Irina Cirpus[1], Jolein Gloerich[2], Wim Geerts[1], Huub J. M. Op den Camp[1], Harry R. Harhangi[1], Eva M. Janssen-Megens[3], Kees-Jan Francoijs[3], Hendrik G. Stunnenberg[3], Jan T. Keltjens[1], Mike S. M. Jetten[1,4] & Marc Strous[1,5]

Two distinct microbial processes, denitrification and anaerobic ammonium oxidation (anammox), are responsible for the release of fixed nitrogen as dinitrogen gas (N_2) to the atmosphere[1–4]. Denitrification has been studied for over 100 years and its intermediates and enzymes are well known[5]. Even though anammox is a key biogeochemical process of equal importance, its molecular mechanism is unknown, but it was proposed to proceed through hydrazine (N_2H_4)[6,7]. Here we show that N_2H_4 is produced from the anammox substrates ammonium and nitrite and that nitric oxide (NO) is the direct precursor of N_2H_4. We resolved the genes and proteins central to anammox metabolism and purified the key enzymes that catalyse N_2H_4 synthesis and its oxidation to N_2. These results present a new biochemical reaction forging an N–N bond and fill a lacuna in our understanding of the biochemical synthesis of the N_2 in the atmosphere. Furthermore, they reinforce the role of nitric oxide in the evolution of the nitrogen cycle.

Ammonium is difficult to activate in the absence of molecular oxygen. Therefore, how anammox bacteria are able to oxidize ammonium coupled to the reduction of nitrite and forge an N–N bond to make N_2 has been an intriguing question for a long time. Based on the *in silico* analysis of the genome assembly of the anammox bacterium *Kuenenia stuttgartiensis*, a set of three redox reactions (equations (1)–(3)) involving N_2H_4 and nitric oxide (NO) was proposed[6] to explain the overall anammox stoichiometry (equation (4)):

$$NO_2^- + 2H^+ + e^- = NO + H_2O \ (E_0' = +0.38\ V) \quad (1)$$

$$NO + NH_4^+ + 2H^+ + 3e^- = N_2H_4 + H_2O \ (E_0' = +0.06\ V) \quad (2)$$

$$N_2H_4 = N_2 + 4H^+ + 4e^- \ (E_0' = -0.75\ V) \quad (3)$$

$$NH_4^+ + NO_2^- = N_2 + 2H_2O \ (\Delta G^{o\prime} = -357\ kJ\ mol^{-1}) \quad (4)$$

The role of N_2H_4 in anammox catabolism was originally proposed based on the observation that the compound transiently accumulated when anammox bacteria were incubated with millimolar quantities of hydroxylamine[7,8]. However, the turnover of neither N_2H_4, hydroxylamine nor NO was demonstrated to start from the actual substrates ammonium and nitrite; thus it remained unclear whether the observed reaction was an integral part of the anammox pathway or a side reaction.

In the present study, we resolved the anammox pathway and its enzymes by a combination of complementary approaches (Fig. 1). *K. stuttgartiensis* was enriched and grown as suspended cells in a membrane bioreactor[9,10]. Fluorescence *in situ* hybridization (FISH) showed that *K. stuttgartiensis* made up more than 95% of the population. Transcription was shown for more than 97% of all genes after random hexamer-primed reverse transcription of extracted RNA, sequencing and mapping of 5.6 million 32-nucleotide reads on an Illumina Genome Analyser (metatranscriptome accession number GSE15408). Expression of 1010 proteins was demonstrated by metaproteomics[11] (peptidome accession number PSE111). Further, inhibitor and isotope labelling studies were performed and the activity of enzyme complexes was demonstrated after their purification by liquid chromatography.

Transcriptomics and proteomics indicated that *K. stuttgartiensis* expressed cd_1 nitrite::nitric oxide reductase (NirS, kuste4136, 9% of predicted peptides detected (p.p.d.) and 6.3-fold messenger RNA (mRNA) coverage) with the potential ability to reduce nitrite to NO. This possibility was investigated by incubating cell suspensions of *K. stuttgartiensis* with ammonium, nitrite (2 mM each) and 100 μM NO scavenger PTIO (2-phenyl-4,4,5,5,-tetramethylimidazoline-1-oxyl-3-oxide)[12]. When PTIO was introduced at the start of the incubation or when it was added to active cells, anammox activity was inhibited (Fig. 2a). Further, the cells were incubated with ammonium and nitrite (2 mM each) in the presence of DAF2-DA (10 μM) that reacts with NO to form a fluorescent product[13,14]. Sampled *K. stuttgartiensis* cells displayed the characteristic green fluorescence indicating NO production (Fig. 2b and Supplementary Fig. 1). In control experiments without nitrite or with added PTIO, there was no detectable fluorescent signal. It should be noted that both PTIO and DAF2-DA might have a wider reaction spectrum than NO and might

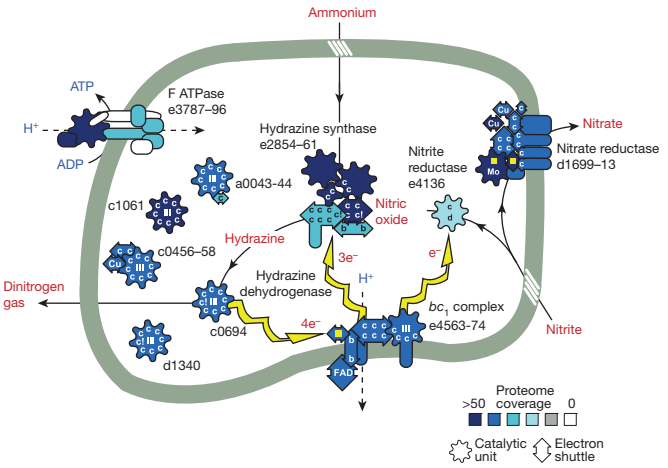

Figure 1 | Biochemical pathway and enzymatic machinery of *K. stuttgartiensis*. The anammoxosome, an intracytoplasmic compartment bounded by a membrane (grey line), is the locus of anammox catabolism. Identifiers of open reading frames and the degree to which the encoded respiratory protein complexes were detected in the proteome are indicated. Hydrazine synthase depicted in the centre of the figure is also loosely membrane associated. Yellow arrows, electron flow; yellow square, iron–sulphur clusters; b, haem b; c, haem c; c!, atypical haem c; d, haem d; Mo, molybdopterin. Cofactors and motifs were determined previously[6].

[1]Institute for Water and Wetland Research, Department of Microbiology, Radboud University Nijmegen, Heyendaalseweg 135, 6525AJ Nijmegen, The Netherlands. [2]Nijmegen Centre for Mitochondrial Disorders, Nijmegen Proteomics Facility, Department of Laboratory Medicine, Radboud University Nijmegen Medical Centre, Geert Grooteplein 10, 6500HB Nijmegen, The Netherlands. [3]Radboud University, Department of Molecular Biology, Nijmegen Centre for Molecular Life Sciences, Geert Grooteplein 28, 6525 GA Nijmegen, The Netherlands. [4]Delft University of Technology, Department of Biotechnology, 2628 BC Delft, The Netherlands. [5]Max Planck Institute for Marine Microbiology, Celsiusstrasse 1, 28359 Bremen, Germany.

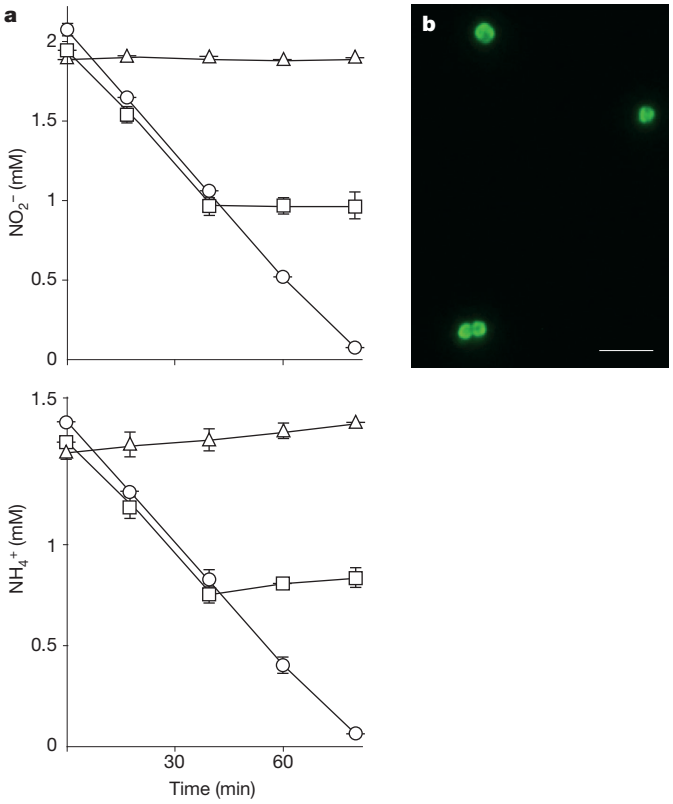

Figure 2 | Determination of nitric oxide (NO) as an intermediate. NO_2^- and NH_4^+ (2 mM each) conversion was inhibited by 100 μM PTIO (**a**). PTIO added at $t = 0$ (open triangle), PTIO added at 40 min (open square) and without PTIO (open circle), $n = 2$ (error bars, s.d.). (**b**) Epifluorescence image of (diaminofluorescein-2-diacetate) DAF2-DA derivative of NO formed during NH_4^+ and NO_2^- (2 mM each) conversion by anammox bacteria (scale bar, 10 μm).

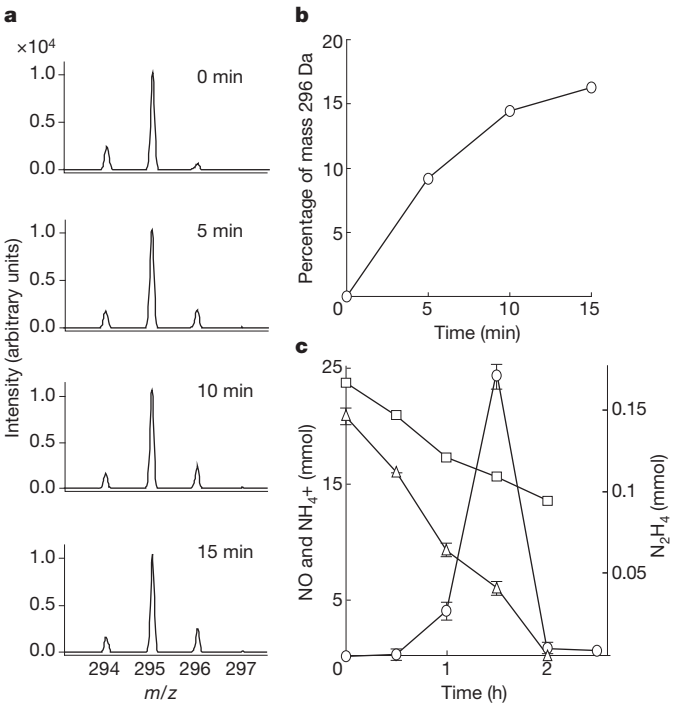

Figure 3 | Hydrazine turnover. *K. stuttgartiensis* cells were incubated with 2 mM $^{15}NO_2^-$ and $^{14}NH_4^+$ each in the presence of 2 mM $^{28}N_2H_4$. Under these conditions cells would only produce $^{29}N_2H_4$ and preferentially consume $^{28}N_2H_4$, leading to ^{15}N-label accumulation in the N_2H_4 pool. The 295 and 296 *m/z* masses correspond to derivatization products of $^{28}N_2H_4$ and $^{29}N_2H_4$ with *para*-dimethylaminobenzaldehyde[30] (**a**). The 294 *m/z* mass arises from the impurities of the matrix. Within 15 min, 16% of the N_2H_4 pool was labelled (**b**). Hydrazine (open circles) was produced by the cells incubated with 2 mM NH_4^+ (open triangles) and NO (0.1 mM) (open squares), $n = 2$ (error bars, s.d.) (**c**).

possibly react with other nitrogen monoxides such as nitroxyl (HNO). However, unlike NO, HNO was not a suitable substrate for hydrazine synthase (see below).

Interestingly, when acetylene (15 μM) was added, the anammox reaction was inhibited. Acetylene inhibits aerobic ammonium oxidation by binding covalently to the ammonia monooxygenase, the ammonia-activating enzyme of aerobic ammonium oxidizers[15–17]. Apparently, it also interfered with the ammonium-activating step of anammox cells (equation (2)). Importantly, acetylene inhibition resulted in an immediate accumulation of NO; hydroxylamine accumulation was not observed, consistent with the role of NO as the direct precursor for N_2H_4.

The second step of the predicted anammox pathway would then be the reduction of NO and its simultaneous condensation with ammonium to produce N_2H_4 (equation (2)). Because the role of N_2H_4 in anammox catabolism was not established, we first demonstrated its *in vivo* turnover (Fig. 3a, b). To investigate whether N_2H_4 could be produced directly from NO, cell suspensions were incubated with NO (0.1 mM) and ammonium (2 mM). A transient accumulation of hydrazine (18 μM) was observed (Fig. 3c), albeit at a much lower concentration (200–500 μM) for incubations with hydroxylamine[7,8]. This is consistent with equations (1)–(3) because the major part of the produced N_2H_4 would be oxidized to N_2 as expected from the overall reaction and NO could be supplied at much lower concentrations (equation (5)).

$$NO + NH_4^+ = \tfrac{1}{4}N_2H_4 + H_2O + \tfrac{3}{4}N_2 + H^+ \qquad (5)$$

The anammox pathway is completed by the oxidation of N_2H_4 to N_2 (equation (3)). For a long time, N_2H_4 was known as an alternative substrate for octahaem hydroxylamine oxidoreductases (HAOs), the enzymes that catalyse the conversion of hydroxylamine to nitrite in aerobic ammonium oxidizers[18,19]. Strikingly, the *K. stuttgartiensis* genome encoded ten divergent paralogues of this enzyme, and six were detected at high levels in the transcriptome and proteome (mRNA up to 189-fold coverage, 27–58% p.p.d.; Supplementary Table 1). Six expressed paralogues belonged to the 'type II' hydrazine/hydroxylamine oxidoreductases (HZO/HAO)[20]. Two related 'type II' HZO/HAO and one divergent octahaem cytochrome *c* were also detected at lower levels (4–15% p.p.d.) and one was not detected. By a two-step liquid chromatography procedure, we purified two highly expressed HZO/HAO-like proteins (kustc0694 and kustc1061). These enzymes appear to be closely related to two enzymes of unknown function isolated from an anammox enrichment culture KSU-1 (refs 21, 22). Both enzymes catalysed the four-electron oxidation of N_2H_4 to N_2 with cytochrome *c* as the artificial electron acceptor with different rates (2.5 and 0.4 μmol min^{-1} mg $protein^{-1}$, respectively). When they were incubated with $^{30}N_2H_4$ and cytochrome *c*, $^{30}N_2$ ($^{15}N^{15}N$) was produced stoichiometrically, in agreement with equation (3). Interestingly, Kustc1061 also oxidized hydroxylamine to NO (rather than nitrite) with a higher rate (6 μmol min^{-1} mg $protein^{-1}$). In contrast, kustc0694 did not catalyse this reaction and hydroxylamine and NO were powerful inhibitors of N_2H_4 oxidation, suggesting kustc0694 was the dedicated hydrazine dehydrogenase (HDH) in *K. stuttgartiensis*. Furthermore, the inhibition of kustc0694 explained the transient accumulation of N_2H_4 in the presence of hydroxylamine or NO.

Although no enzyme is known to convert NO and ammonium into N_2H_4, two candidate gene clusters were previously identified potentially encoding an enzyme complex with this function (hydrazine synthase, HZS)[6]. One of these clusters (kuste2859–61) encoded the

most highly expressed proteins in the proteome (greater than 60% p.p.d., visible as three dominant spots on two-dimensional gels; Supplementary Table 1 and Supplementary Fig. 2a) and extremely abundant mRNAs in the transcriptome (greater than 50-fold coverage). The transcription of the other candidate cluster (kuste2474–83) was well below average (1.7-fold coverage) and expression was not detected by proteomics.

The kuste2859–61 proteins were purified from the cell-free extract of the *K. stuttgartiensis* as a complex that separated into three distinct bands on a denaturing polyacrylamide gel, corresponding to polypeptides encoded by three consecutive genes (kuste2859–2860–2861, Supplementary Fig. 2). Native polyacrylamide gel electrophoresis revealed that the complex was a multimer of approximately 240 kDa. Hydrazine synthesis activity of the complex was shown in a coupled assay with the kustc1061 HZO/HAO, using ^{15}N-ammonium (1 mM) and NO (0.9 mM) as substrates (Fig. 4). In the assay, kustc1061 would 'pull' the reaction by rapidly oxidizing the produced N_2H_4 to $^{29}N_2$ as the end product, while simultaneously 'pushing' the reaction by providing the electrons for N_2H_4 synthesis (equations (2) and 3). Kustc1061 alone did not catalyse the reaction, and N_2 production above background could not be measured in the absence of ammonium or NO. N_2 was not produced above background when hydroxylamine or nitroxyl (HNO) were provided as substrates with ammonium. The activity of N_2 formation in the coupled assay was 20 nmol h^{-1} mg protein^{-1}, lower than the activity of whole cells with ammonium and nitrite (approximately 1800 nmol h^{-1} mg protein^{-1}). The cell-free extracts were unable to form N_2 from ammonium and nitrite, but could from NO and ammonium under the same experimental conditions, at six-fold lower rate than the purified HZS (3.4 nmol h^{-1} mg protein^{-1}). The decrease in activity upon mere cell disruption was most probably due to the disruption of a tightly coupled multi-component system with hydrazine synthesis as the rate-limiting step.

Interestingly, the kuste2859–61 complex was capable of N_2 formation from ammonium and NO on its own (Fig. 4). The purified enzyme oxidized N_2H_4 to N_2 with a specific activity of 34 nmol min^{-1} mg protein^{-1}, resulting in an overall disproportionation reaction (equation (5)). Considering that N_2H_4 is the energy source in anammox

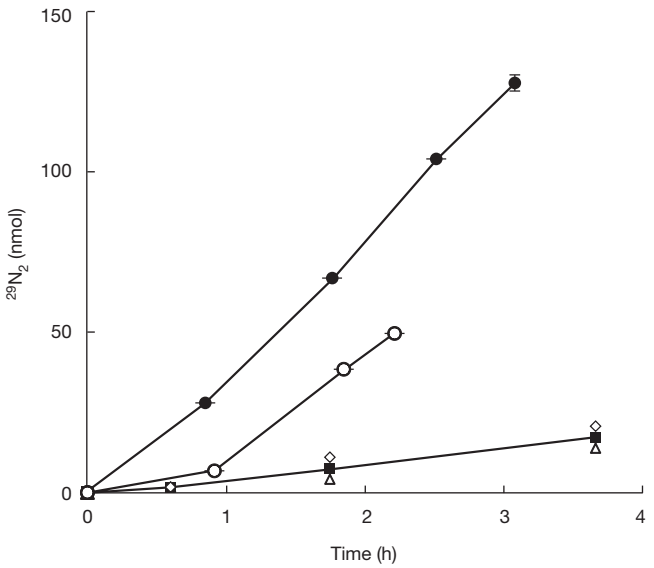

Figure 4 | $^{29}N_2$ production by hydrazine synthase complex and kustc1061 from $^{15}NH_4^+$ and NO. $^{29}N_2$ was produced with the highest rate when hydrazine synthase complex (1.6 mg) and kustc1061 (4.7 μg) was incubated with $^{15}NH_4^+$ (1 mM), ^{14}NO (0.9 mM) and cytochrome *c* (50 μM) (filled circles). In the control experiments, hydrazine synthase complex and cytochrome *c* (open circles), kustc1061 and cytochrome *c* (open diamonds), cytochrome *c* (filled squares) and only buffer (open triangles) were incubated under the same experimental conditions; $n = 3$ (error bars, s.d.).

metabolism, N_2 formation by HZS would be unproductive. Consequently, we may speculate that the anammox bacterium harbours backup systems that efficiently trap hydrazine and that keep (nitrogenous) inhibitory compounds, like NO and hydroxylamine, at low concentrations, which would partly explain the redundancy of HAO/HZO-like proteins in the organism. Our experiments showed that HZS and HDH were necessary and sufficient to make N_2 from the substrate ammonium and the intermediate NO.

Taken together, anammox catabolism and energy for growth must be conserved from three reactions (equations (1)–(3)). It is hypothesized that anammox bacteria synthesize ATP through a membrane-bound ATP synthase complex driven by proton-motive force (pmf) generated through catabolic reactions with the intermediary action of the quinol::cytochrome *c* oxidoreductase system (complex III, the bc_1 complex).

Intriguingly, three gene clusters encoding bc_1 complexes and four encoding ATP synthases were present in the *K. stuttgartiensis* genome. Transcription and expression of one (kuste4569–74) of these gene clusters were detected at higher levels (26–33% p.p.d., 6- to 24-fold mRNA coverage) than the other two (0–19% p.p.d., 2- to 15-fold mRNA coverage). When *K. stuttgartiensis* cell suspensions were spiked with pentachlorophenol (10 μM), a structural analogue of quinol and a known inhibitor of the bc_1 complex, anammox activity was completely inhibited, indicating that the bc_1 complex was involved in energy conservation and its role in electron transport from N_2H_4 oxidation to nitrite reduction and hydrazine synthesis was not backed up by any other system. The expression of the four gene clusters encoding ATP synthase was even more skewed. Peptide coverage for kuste3789–96 was 14–58% p.p.d. compared with less than 1% for the other three ATP synthases, and mRNA coverage differed by a factor of six. The gene product encoding the catalytic β-subunit of the highest expressed ATP synthase (kuste3787–96) was recently shown to be associated with the membranes of the intracellular cell compartment, the anammoxosome, suggesting it to be the site where the proton-motive machinery resides[23].

In the present study we experimentally identified NO and N_2H_4 as the intermediates of anaerobic ammonium oxidation. The highly expressed protein encoded by the gene cluster kuste2859–61 was purified and N–N bond formation from NO and ammonium was demonstrated. Hydrazine synthase and the NO reductase of denitrifiers are the two enzymes capable of bonding two N atoms together. In contrast to NO reductase, hydrazine synthase combines two different nitrogenous molecules. It is intriguing that all the N_2 in our atmosphere is formed by the oxidizing power of NO, in line with the hypothesis that NO may have been the first deep redox sink on Earth[24].

METHODS SUMMARY

Activity Measurements. Physiological experiments were performed at 33 °C, pH 7.5 with *K. stuttgartiensis* cells[9,10]. To determine the role of NO and hydroxylamine in the anammox metabolism, cells were incubated with (1) $NaNO_2$, NH_4Cl (2 mM each) and spiked with acetylene (15 μM); (2) $NaNO_2$, NH_4Cl (2 mM each) and DAF-2DA (10 μM) or PTIO (100 μM); (3) NO (0.1 mM) and 2 mM NH_4Cl. Hydroxylamine, NH_4^+, NO_2^- and N_2H_4 were determined as previously described[25,26]. NO was measured online as previously described[27]. To determine N_2H_4 turnover, cells were incubated with $Na^{15}NO_2$, NH_4Cl (or vice versa) and N_2H_4 (2 mM each). Isotopic composition of hydrazine was determined with matrix-assisted laser desorption/ionization–time of flight mass spectroscopy (MALDI–TOF MS) after *para*-dimethylaminobenzaldehyde derivatization, developed after Watt and Chrisp[25]. All labelled compounds were 99% pure (Cambridge Isotope Laboratories).

Proteins were purified from cell-free extracts with anion exchange and hydroxyapatite liquid chromatography. Activity measurements were performed at 37 °C, pH 7 in an anaerobic chamber. Kuste2859–61 (1.6 mg) and kustc1061 (4.7 μg) were incubated with NO (0.9 mM) and $^{15}NH_4Cl$ (1 mM), and $^{29}N_2$ production was monitored by gas chromatography (Agilent 6890 with a PorapakQ column, 80 °C) combined with a mass spectrometer (Agilent 5975c quadruple inert MS). For rate calculations, kustc0694 (1.3 μg) or kustc1061 (4.7 μg) were

incubated with N_2H_4 or hydroxylamine and cytochrome *c* (50 μM each), and $^{30}N_2$ or ^{31}NO production was measured.

Molecular methods. Total RNA was extracted, reverse transcribed, sequenced with Illumina and mapped to the genome sequence of *K. stuttgartiensis*[6]. From the aligned reads, per-position coverage was calculated for each contig and used to calculate the coverage for each orf, intergenic region and predicted RNA element.

Cell free extracts were separated by SDS–polyacrylamide gel electrophoresis (SDS–PAGE) or two-dimensional gel electrophoresis, digested with trypsin and analysed with liquid chromatography–mass spectrometry (LC–MS/MS)[28,29]. Mass spectrometry data was searched against a database of predicted *K. stuttgartiensis* peptide sequences.

Full Methods and any associated references are available in the online version of the paper at www.nature.com/nature.

Received 30 May; accepted 12 August 2011.
Published online 2 October 2011.

1. Arrigo, K. R. Marine microorganisms and global nutrient cycles. *Nature* **437,** 349–355 (2005).
2. Brandes, J. A., Devol, A. H. & Deutsch, C. New developments in the marine nitrogen cycle. *Chem. Rev.* **107,** 577–589 (2007).
3. Payne, W. J. Reduction of nitrogenous oxides by microorganisms. *Bacteriol. Rev.* **37,** 409–452 (1973).
4. Strous, M. *et al.* Missing lithotroph identified as new planctomycete. *Nature* **400,** 446–449 (1999).
5. Zumft, W. G. Cell biology and molecular basis of denitrification. *Microbiol. Mol. Biol. Rev.* **61,** 533–616 (1997).
6. Strous, M. *et al.* Deciphering the evolution and metabolism of an anammox bacterium from a community genome. *Nature* **440,** 790–794 (2006).
7. Van de Graaf, A. A., deBruijn, P., Robertson, L. A., Jetten, M. S. M. & Kuenen, J. G. Metabolic pathway of anaerobic ammonium oxidation on the basis of N-15 studies in a fluidized bed reactor. *Microbiology* **143,** 2415–2421 (1997).
8. Kartal, B. *et al.* Candidatus 'Brocadia fulgida': an autofluorescent anaerobic ammonium oxidizing bacterium. *FEMS Microbiol. Ecol.* **63,** 46–55 (2008).
9. Kartal, B., Geerts, W. & Jetten, M. S. M. Cultivation, detection and ecophysiology of anaerobic ammonium-oxidizing bacteria. *Methods Enzymol.* **486,** 89–108 (2011).
10. Van der Star, W. R. L. *et al.* The membrane bioreactor: a novel tool to grow anammox bacteria as free cells. *Biotechnol. Bioeng.* **101,** 286–294 (2008).
11. Keller, M. & Hettich, R. Environmental proteomics: a paradigm shift in characterizing microbial activities at the molecular level. *Microbiol. Mol. Biol. Rev.* **73,** 62–70 (2009).
12. Akaike, T. & Maeda, H. Quantitation of nitric oxide using 2-phenyl-4,4,5,5-tetramethylimidazoline-1-oxyl 3-oxide (PTIO). *Methods Enzymol.* **268,** 211–221 (1996).
13. Guo, F. Q., Okamoto, M. & Crawford, N. M. Identification of a plant nitric oxide synthase gene involved in hormonal signaling. *Science* **302,** 100–103 (2003).
14. Nagano, T. Practical methods for detection of nitric oxide. *Luminescence* **14,** 283–290 (1999).
15. Gilch, S., Vogel, M., Lorenz, M. W., Meyer, O. & Schmidt, I. Interaction of the mechanism-based inactivator acetylene with ammonia monooxygenase of *Nitrosomonas europaea*. *Microbiology* **155,** 279–284 (2009).
16. Hyman, M. R. & Wood, P. M. Suicidal inactivation and labeling of ammonia mono-oxygenase by acetylene. *Biochem. J.* **227,** 719–725 (1985).
17. McTavish, H., Fuchs, J. A. & Hooper, A. B. Sequence of the gene coding for ammonia monooxygenase in *Nitrosomonas europaea*. *J. Bacteriol.* **175,** 2436–2444 (1993).
18. Hooper, A. B. & Nason, A. Characterization of hydroxylamine-cytochrome c reductase from chemoautotrophs *Nitrosomonas europaea* and *Nitrosocystis oceanus*. *J. Biol. Chem.* **240,** 4044–4057 (1965).
19. Hooper, A. B., Vannelli, T., Bergmann, D. J. & Arciero, D. M. Enzymology of the oxidation of ammonia to nitrite by bacteria. *Anton. Leeuw. Int. J. G. Microbiology* **71,** 59–67 (1997).
20. Klotz, M. G. *et al.* Evolution of an octahaem cytochrome c protein family that is key to aerobic and anaerobic ammonia oxidation by bacteria. *Environ. Microbiol.* **10,** 3150–3163 (2008).
21. Shimamura, M. *et al.* Isolation of a multiheme protein with features of a hydrazine-oxidizing enzyme from an anaerobic ammonium-oxidizing enrichment culture. *Appl. Environ. Microbiol.* **73,** 1065–1072 (2007).
22. Shimamura, M. *et al.* Another multiheme protein, hydroxylamine oxidoreductase, abundantly produced in an anammox bacterium besides the hydrazine-oxidizing enzyme. *J. Biosci. Bioeng.* **105,** 243–248 (2008).
23. Van Niftrik, L. *et al.* Intracellular localization of membrane-bound ATPases in the compartmentalized anammox bacterium '*Candidatus* Kuenenia stuttgartiensis'. *Mol. Microbiol.* **77,** 701–715 (2010).
24. Ducluzeau, A. L. *et al.* Was nitric oxide the first deep electron sink? *Trends Biochem. Sci.* **34,** 9–15 (2009).
25. Watt, G. W. & Chrisp, J. D. A spectrophotometric method for the determination of hydrazine. *Anal. Chem.* **24,** 2006–2008 (1952).
26. Strous, M., Heijnen, J. J., Kuenen, J. G. & Jetten, M. S. M. The sequencing batch reactor as a powerful tool for the study of slowly growing anaerobic ammonium-oxidizing microorganisms. *Appl. Microbiol. Biotechnol.* **50,** 589–596 (1998).
27. Kartal, B. *et al.* Effect of nitric oxide on anammox bacteria. *Appl. Environ. Microbiol.* **76,** 6304–6306 (2010).
28. Rappsilber, J., Ishihama, Y. & Mann, M. Stop and go extraction tips for matrix-assisted laser desorption/ionization, nanoelectrospray, and LC/MS sample pretreatment in proteomics. *Anal. Chem.* **75,** 663–670 (2003).
29. Wilm, M. *et al.* Femtomole sequencing of proteins from polyacrylamide gels by nano-electrospray mass spectrometry. *Nature* **379,** 466–469 (1996).
30. Audrieth, L. F. & Ackerson Ogg, B. *The Chemistry of Hydrazine* (Wiley, 1951).

Supplementary Information is linked to the online version of the paper at www.nature.com/nature.

Acknowledgements B.K. was supported by a grant (05987) from the Dutch Foundation for Applied Research. W.J.M. was supported by a grant (142161201) from the Darwin Center for Biogeosciences. N.M.d.A. and I.C. were supported by a grant (81802015) from the Netherlands Organization for Scientific Research. M.S. was supported by a VIDI grant from the Netherlands Organization for Scientific Research and a European Research Council grant MASEM (242635). The anammox research of M.S.M.J. is supported by an advanced grant (232987) from the ERC. The authors acknowledge R. Klefoth for the initial tests for protein purification procedures.

Author Contributions Physiological experiments were conceived, designed and performed by B.K., *Kuenenia stuttgartiensis* was grown by B.K. and W.G., two-dimensional gel electrophoresis was performed by N.M.A. and I.C., one-dimensional gel electrophoresis was performed by W.J.M. and B.K., MALDI–TOF analysis was performed by B.K., W.J.M. and H.J.M.O.d.C., nanoLC-MS/MS by J.G., RNA extraction and reverse transcription by H.R.H., Illumina sequencing by E.M.J.-M., K.-J.F. and H.S., and protein purification and activity tests were designed by W.J.M., B.K. and J.T.K. and performed by W.J.M. Proteomic and transcriptomic data processing was performed by J.G., M.S., K.-J.F., B.K., M.S.M.J. and H.J.M.O.d.C. The manuscript was written by B.K. with input from J.T.K., M.S. and M.S.M.J.

Author Information The metatranscriptome and peptidome sequences are deposited in Gene Expression Omnibus under accession numbers GSE15408 and PSE111, respectively. Reprints and permissions information is available at www.nature.com/reprints. The authors declare no competing financial interests. Readers are welcome to comment on the online version of this article at www.nature.com/nature. Correspondence and requests for materials should be addressed to B.K. (kartal@science.ru.nl).

METHODS

Source of the biomass. *K. stuttgartiensis* cells were collected from a 10-l laboratory scale anammox membrane bioreactor[9,10] and were concentrated by centrifugation. The cells were re-suspended to a protein concentration higher than 1 mg ml^{-1}. Part of the cell suspension was diluted 100 times, chemically fixed, and hybridizations with fluorescently labelled oligonucleotide probes were performed as described previously[31,32].

Sample preparation. The cell suspensions were transferred to 8-ml serum bottles. The vials were made anoxic by alternately applying under-pressure and He or Ar seven times and were transferred to an anaerobic chamber with a 95%/5% Ar/H_2 atmosphere. O_2 in the Ar in the anaerobic chamber was removed by passing Ar over a Pd catalyst (0.2 p.p.m. residual O_2). In the anaerobic chamber, cell suspensions were diluted five times with anaerobic mineral medium[33] (pH 7.5) to a final volume of 40 or 8 ml and transferred to glass vials unless stated otherwise. All preparations (for example, addition of substrates and/or inhibitors) for different incubations were handled in the anaerobic chamber. All experiments were performed at least in duplicate. All non-labelled salts were purchased as molecular grade (more than 99.95% pure, Merck) unless stated otherwise. All labelled compounds were 99% pure and purchased as sodium or chloride salts (Cambridge Isotope Laboratories). All gaseous compounds were of the highest purity available.

Analytical methods. NO_2^- and NH_4^+ were determined as described previously[27]. N_2H_4 was determined colourimetrically at 420 nm after reaction of 100-µl sample with 900 µl 2% (w/v) *para*-dimethylaminobenzaldehyde (PDB), 3.7% (v/v) HCl in ethanol[30]. NH_2OH (detection limit 5 µM) was determined as previously described[27].

Effect of PTIO. To determine the effect of PTIO, an NO scavenger[12], on anammox bacteria, three incubations were performed in parallel. NO_2^- and NH_4^+ (2 mM) were added to all incubations. To the first incubation, PTIO (100 µM) was added at 0 min, to the second it was added at 40 min, and no PTIO was added to the third incubation. Liquid samples were taken every 15 min and analysed for NH_4^+, NO_2^- and NH_2OH as previously described[27].

Bioimaging of nitric oxide. To detect NO turnover, *K. stuttgartiensis* cell suspensions were incubated with 2 mM NO_2^- and NH_4^+ in amber vials. In parallel, nitrite-depleted cell suspensions were incubated in the presence of 2 mM NH_4^+. After a 5-min pre-incubation, diaminofluorescein-2-diacetate (DAF2-DA, Calbiochem) was added to a final concentration of 10 µM. The vials were incubated in the dark for 30 min at 33 °C and were shaken continuously at 300 r.p.m. As a negative control, cells were incubated with PTIO and DAF2-DA. Cells were then harvested by centrifugation, washed three times in mineral medium[33] to remove the excess chromophore and were re-suspended in mineral medium. A liquid sample (5 µl) of the suspension was pipetted on a microscope slide and dried in the dark. The preparations were examined with a Zeiss Axioplan2 epifluorescence microscope.

Batch experiments. To determine the activity of *K. stuttgartiensis* with NO and NH_4^+, cell suspensions were incubated with NO (0.1 mM) and 2 mM NH_4^+ in 100-ml glass vials with 10% NO (in He) in the headspace. Gas samples were analysed in a chemoilluminescence NO_x analyser (CLD 700EL, EcoPhysics, detection limit 0.1 p.p.m. NO). Liquid samples were taken every 30 min and analysed for NH_4^+ and N_2H_4 as previously described[27,30].

To determine the effect of acetylene on anammox bacteria, *K. stuttgartiensis* suspensions were transferred to 40-ml glass vials. NO_2^- and NH_4^+ were added to the incubations to a final concentration of 2 mM. The vials were incubated at 33 °C and were mixed with a magnetic stirrer at 500 r.p.m. and continuously flushed with Ar/CO_2 (95%/5%) with a flow of 10 ml min^{-1}. The effluent gas from the vials was connected to a chemoilluminescence NO_x analyser (CLD 700EL, EcoPhysics, detection limit 0.1 p.p.m. NO) for online NO measurement. At 15 min, 100 µl acetylene (15 µM) was added to the vials. As negative controls, 100 µl air and 100 µl nitrogen were added to separate incubations. Liquid samples were taken from the incubations every 10–15 s and chilled to 0 °C immediately. The supernatant of each sample was transferred to an Eppendorf cup and kept at 4 °C until they were analysed for NH_4^+, N_2H_4 and NH_2OH.

Detection of hydrazine turnover in anammox cells. To detect N_2H_4 turnover, $^{15}NO_2^-$, NH_4^+ (or vice versa) and N_2H_4 (2 mM each) were added to the *K. stuttgartiensis* cell suspensions. The vials were incubated in the dark for 15 min at 30 °C, 300 r.p.m. Liquid samples were taken every 5 min, and isotopic composition of N_2H_4 was determined by MALDI–TOF MS after reaction with PDB. For MALDI–TOF analysis, 10 µl of PDB-reacted samples were mixed with an equal volume of sample buffer containing 20 mg ml^{-1} α-cyano-4-hydroxycinnamic acid in 0.05% (v/v) trifluoroacetic acid (TFA), 50% (v/v) acetonitrile. The mixtures (0.3 µl) were spotted on a S26/100 M-probe (Bruker 15165), which was inserted into a multiprobe adaptor. MALDI–TOF MS measurements were performed in the mass range of 100–800 Da on a Bruker III mass spectrometer, using the reflectron mode.

Cytochrome bc_1 complex. To determine the role of cytochrome bc_1 complex in anammox catabolism, *K. stuttgartiensis* suspensions were incubated with pentachlorophenol, a specific inhibitor of the bc_1 complex. NO_2^- and NH_4^+ were added to the incubations to a final concentration of 2 mM. Pentachlorophenol was added to a final concentration of 10 µM. NO_2^- and NH_4^+ were determined as described previously[27].

Preparation of cell free extract. *K. stuttgartiensis* cells (2 l, OD_{600} 1.2) were harvested from the membrane bioreactor. After centrifugation (4,000*g*, 4 °C), the pellet was re-suspended in one volume 20 mM potassium phosphate buffer, pH 8. Cell suspensions were passed three times through a French pressure cell operated at 138 MPa. The lysate was incubated with 1% (w/v) sodium deoxycholate at 4 °C for 1 h to solubilize membrane associated proteins. After centrifugation for 15 min at 1,700*g* at 4 °C, the cell-free fraction was obtained as clarified supernatant.

Protein electrophoresis and MALDI–TOF analysis. Samples were denatured by incubation with 60 mM Tris-HCl buffer (pH 8) containing 5% β-mercaptoethanol, 2% SDS (sodium dodecyl sulphate) and 25% glycerol for 5 min at 100 °C. SDS–PAGE was performed in 10% or 6% slab gels in 375 mM Tris-HCl glycine buffer, pH 8.8 according to Laemmli[34]. Native PAGE (6%) was performed according to the same procedure with the following modifications: the protein preparations were not boiled before electrophoresis, SDS and β-mercaptoethanol were omitted from the gels, and Tris-HCl glycine (375 mM, pH 8.3) was used as the running buffer. Gels were stained with colloidal Coomassie blue as described elsewhere[35]. To identify the protein bands resolved in SDS–PAGE, gel spots (~3 mm^3) were picked, digested with trypsin and analysed with MALDI–TOF mass spectrometry as described elsewhere[36].

Purification of kuste2859–2860–2861, kustc0694 and kustc1061. Cell-free extract was centrifuged at 140,000*g*, 10 °C (Discovery 10, Sorvall, equipped with a T-1270 rotor) to remove the membranes. The supernatant was loaded on a 30 ml Q Sepharose XL (GE Healthcare) column equilibrated with 20 mM Tris-HCl, pH 8. Kuste2859–2860–2861 and kustc1061 were eluted isocratically with 200 mM NaCl in 20 mM Tris-HCl, pH 8 (2 ml min^{-1}). Kustc0694 was eluted isocratically with 400 mM NaCl in 20 mM Tris-HCl, pH 8 (2 ml min^{-1}). Eluted fractions were subsequently loaded onto a 10 ml Hydroxyapatite (Bio-Rad) column equilibrated with 20 mM potassium phosphate buffer, pH 7 and eluted with a gradient of the same buffer (20–500 mM, 2 ml min^{-1}). Kustc1061 and kuste2859–2860–2861 were collected in fractions eluted at 100 mM and 200 mM phosphate, respectively. The pooled fractions were desalted and concentrated using Vivaspin tubes (100 kDa cut-off, Sartorius Stedim Biotech) to concentrations of at least 0.86 mg ml^{-1} (kuste2859–2860–2861) and 2.3 mg ml^{-1} (kustc1061) in 20 mM phosphate buffer, pH 7.

Detection of hydrazine and hydroxylamine oxidation by kustc1061 and kustc694. To 2 ml (final volume) of phosphate buffer (20 mM, pH 7), 4.7 µg of Kustc1061 or 1.3 µg of Kustc0694 and cytochrome *c* (50 µM final concentration, bovine heart, Sigma-Aldrich) were added to a 3-ml exetainer (Labco). To start the reaction to determine the electron stoichiometry, 10 µM, and for routine rate assays 50 µM, ^{15}N-labelled $^{30}N_2H_4$ was added from an anoxic stock. To determine the capacity for NH_2OH oxidation, proteins were incubated in separate vials with 50 µM NH_2OH and cytochrome *c* (each). Exetainers were incubated at 37 °C in the anaerobic chamber. $^{30}N_2$ and ^{15}NO production was monitored by gas chromatography (Agilent 6890 equipped with a Porapak Q column at 80 °C) combined with a mass spectrometer (Agilent 5975c quadruple inert MS).

Combined assay of kuste2859–2860–2861 and kustc1061. Cytochrome *c* (50 µM final concentration, bovine heart, Sigma-Aldrich), Kustc1061 (4.7 µg), 1 mM $^{15}NH_4^+$ and 5 µM N_2H_4 were added to 1.6 mg of kuste2859–2860–2861 in 1 ml phosphate buffer (20 mM, pH 7) in a 3-ml exetainer (Labco). The reaction was started by adding phosphate buffer (20 mM, pH 7) with NO (0.9 mM) to a final volume of 2 ml. Before incubation at 37 °C in the anaerobic chamber, 1 ml of 50% NO (in He) was added to the headspace. Control experiments were performed with ammonium (1 mM) with NH_2OH (1 mM) and HNO supplied as Angeli's salt (41 mM) in separate incubations. $^{29}N_2$ production was monitored by gas chromatography (Agilent 6890 equipped with a Porapak Q column at 80 °C) combined with a mass spectrometer (Agilent 5975c quadruple inert MS).

LC-MS/MS analysis and data processing. After PAGE, gels were stained with colloidal Coomassie blue as described elsewhere[35]. The gel lane was cut into four slices and each slice was destained with three cycles of washing with 50 mM ammoniumbicarbonate and 50% acetonitrile. Protein reduction, alkylation and digestion with trypsin were performed as previously described[30]. After digestion, samples were de-salted and purified according to Rappsilber *et al.*[29]. Sample analysis by LC-MS/MS was performed using an Agilent nanoflow 1100 liquid chromatograph coupled online through a nano-electrospray ion source (Thermo Fisher Scientific) to a 7T linear ion trap Fourier transform ion cyclotron resonance mass spectrometer (LTQ FT, Thermo Fisher Scientific). The chromatographic column consisted of a 15-cm fused silica emitter (New Objective, PicoTip

Emitter, Tip: 8 ± 1 μm, internal diameter 100 μm) packed with 3-μm C18 beads (Reprosil-Pur C18 AQ, Dr Maisch GMBH)[37]. After loading the peptides onto the column in buffer A (0.5% HAc), bound peptides were gradually eluted using a 67-min gradient of buffer B (80% ACN, 0.5% HAc). First, the concentration of acetonitrile was increased from 2.4 to 8% in 5 min, followed by an increase from 8 to 24% acetonitrile in 55 min, and finally an increase from 24 to 40% acetonitrile in 7 min. The mass spectrometer was operated in positive ion mode and was programmed to analyse the top four most abundant ions from each precursor scan using dynamic exclusion. Survey mass spectra (350–2000 m/z) were recorded in the ion cyclotron resonance cell at a resolution of $R = 5E5$. Data-dependent collision-induced fragmentation of the precursor ions was performed in the linear ion trap (normalized collision energy 27%, activation $q = 0.250$, activation time 30 ms).

Mass spectrometric data files were searched against the *K. stuttgartiensis* database (known contaminants like human keratins and trypsin were added to the database) using the database search program Mascot (Matrix Science, version 2.2). To obtain factors for the recalibration of precursor masses, initial searches were performed with a precursor ion tolerance of 50 p.p.m. Fragment ions were searched with 0.8-Da tolerance and searches allowed for one missed cleavage, carbamidomethylation (C) as fixed modification, and deamidation (NQ) and oxidation (M) as variable modifications. The results from these searches were used to calculate the m/z-dependent deviation, which was used to recalibrate all precursor m/z values. After recalibration of the precursor masses, definitive Mascot searches were performed using the same settings as stated above, but with a precursor ion tolerance of 20 p.p.m. Additionally, reverse database searches were performed with the same settings. Protein identifications were validated and clustered using the PROVALT algorithm to achieve a false-discovery rate of less than 1% (ref. 38).

Two-dimentional gel electrophoresis. Before protein separation by isoelectric focusing, 1 mg of the protein suspension was incubated with 1% (v/v) Immobilized pH-gradient (IPG) buffer of the appropriate range, 5 mM tributyl phosphine and 0.01% (w/v) bromophenol blue for 15 min at room temperature and centrifuged at 10,000*g* for 15 min at 10 °C. Isoelectric focusing was performed with the IPGphor system using commercial 24-cm-long IPG strips with linear immobilized pH gradients of various ranges. The conditions for rehydration of the IPG strips, sample entry and isoelectric focusing were as follows: the temperature was set constant at 18 °C and 50-μA per strip were applied.

Focused IPG strips were equilibrated before SDS–PAGE two times for 15 min in 375 mM Tris-HCl pH 8.5, 2% (w/v) SDS, 20% (w/v) glycerol, 6 M urea, 10 mM DTT, 50 mM acrylamide and 0.1% (w/v) bromophenol blue. Gels were run for 45 min with constant cooling to 18 °C at 20 V, 40 W and subsequently at 40 V, 40 W until the bromophenol blue marker reached the end of the gel. Gels were fixed in 30% (v/v) ethanol and 10% (v/v) glacial acetic acid and were stained with colloidal Coomassie blue[39] or silver stain[40]. Picked gel spots were digested and analysed with MALDI–TOF MS as described elsewhere[36].

Blue native PAGE. Blue native PAGE of the protein complexes was performed as described elsewhere[41]. For protein identification in two-dimensional gels, 16 cm × 20 cm gels were self-casted according to Calvaruso *et al.* with the following exception: 4–10% linear polyacrylamide gradient was used[41]. Sample additive (1.5 μl) (0.75 M 6-aminocaproic acid, 5% Serva Blue G) was added to 40 μg protein sample before loading the gel.

Electrophoresis was performed at 50 V until the migration front entered the resolving gel and then at 100 V until the migration front reached the end of the gel. Cathode and anode buffer for blue native PAGE were 50 mM Bis-Tris, pH 7.0, and 50 mM Tricine, 15 mM Bis-Tris, pH 7.0, respectively. Preparation of the first-dimension gel strip and assembly and casting of the second-dimension gel were performed as described elsewhere[41] with the exception that the second-dimension cassette had the same thickness as the first dimension. No Coomassie blue was added to the cathode buffer.

Transcriptomics. RNA was extracted using the Ribopure Bacteria Kit (Ambion) according to the manufacturer's instructions. First-strand cDNA was synthesized with random primers using the RevertAid H Minus First Strand cDNA Synthesis Kit, and the second strand was synthesized using DNA polymerase and manufacturer's instructions (Fermentas).

The quality scores of the obtained Solexa reads (3.5 million) were converted to PHRED format and mapped with Maq (http://maq.sourceforge.net) to the five contigs that constitute the *K. stuttgartiensis* genome (accession numbers CT030148, CT573071–4). From the aligned reads, the per-position coverage was calculated for each contig and used to calculate the coverage for each orf, intergenic region and predicted RNA element.

31. Schmid, M. *et al.* Molecular evidence for genus level diversity of bacteria capable of catalyzing anaerobic ammonium oxidation. *Syst. Appl. Microbiol.* **23,** 93–106 (2000).
32. Schmid, M. C. *et al.* Biomarkers for in situ detection of anaerobic ammonium-oxidizing (anammox) bacteria. *Appl. Environ. Microbiol.* **71,** 1677–1684 (2005).
33. Van de Graaf, A. A., de Bruijn, P., Robertson, L. A., Jetten, M. S. M. & Kuenen, J. G. Autotrophic growth of anaerobic ammonium-oxidizing micro-organisms in a fluidized bed reactor. *Microbiology* **142,** 2187–2196 (1996).
34. Laemmli, U. K. Cleavage of structural proteins during assembly of head of bacteriophage-T4. *Nature* **227,** 680–685 (1970).
35. Candiano, G. *et al.* Blue silver: A very sensitive colloidal Coomassie G-250 staining for proteome analysis. *Electrophoresis* **25,** 1327–1333 (2004).
36. Farhoud, M. H. *et al.* Protein complexes in the archaeon Methanothermobacter thermautotrophicus analyzed by blue native/SDS-PAGE and mass spectrometry. *Mol. Cell. Proteomics* **4,** 1653–1663 (2005).
37. Ishihama, Y., Rappsilber, J., Andersen, J. S. & Mann, M. Microcolumns with self-assembled particle frits for proteomics. *J. Chromatogr. A* **979,** 233–239 (2002).
38. Weatherly, D. B. *et al.* A heuristic method for assigning a false-discovery rate for protein identifications from mascot database search results. *Mol. Cell. Proteomics* **4,** 762–772 (2005).
39. Neuhoff, V., Arold, N., Taube, D. & Ehrhardt, W. Improved staining of proteins in polyacrylamide gels including isoelectric-focusing gels with clear background at nanogram sensitivity using coomassie brilliant blue G-250 and R-250. *Electrophoresis* **9,** 255–262 (1988).
40. Mortz, E., Krogh, T. N., Vorum, H. & Gorg, A. Improved silver staining protocols for high sensitivity protein identification using matrix-assisted laser desorption/ionization-time of flight analysis. *Proteomics* **1,** 1359–1363 (2001).
41. Calvaruso, M. A., Smeitink, J. & Nijtmans, L. Electrophoresis techniques to investigate defects in oxidative phosphorylation. *Methods* **46,** 281–287 (2008).